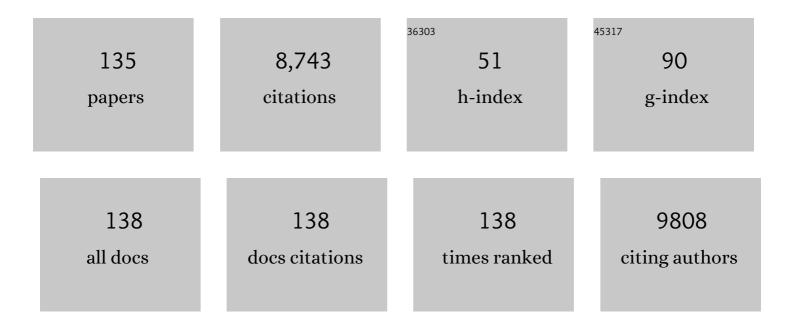
Xiaodong Li

List of Publications by Year in descending order

Source: https://exaly.com/author-pdf/5130098/publications.pdf Version: 2024-02-01



#	Article	IF	CITATIONS
1	Nanoscale Structural and Mechanical Characterization of a Natural Nanocomposite Material:Â The Shell of Red Abalone. Nano Letters, 2004, 4, 613-617.	9.1	545
2	Towards Textile Energy Storage from Cotton T‧hirts. Advanced Materials, 2012, 24, 3246-3252.	21.0	473
3	Biomass-derived renewable carbon materials for electrochemical energy storage. Materials Research Letters, 2017, 5, 69-88.	8.7	402
4	Flexible all-solid-state hierarchical NiCo2O4/porous graphene paper asymmetric supercapacitors with an exceptional combination of electrochemical properties. Nano Energy, 2015, 13, 306-317.	16.0	303
5	In Situ Observation of Nanograin Rotation and Deformation in Nacre. Nano Letters, 2006, 6, 2301-2304.	9.1	294
6	Cotton-textile-enabled flexible self-sustaining power packs via roll-to-roll fabrication. Nature Communications, 2016, 7, 11586.	12.8	282
7	Targeted production of reactive oxygen species in mitochondria to overcome cancer drug resistance. Nature Communications, 2018, 9, 562.	12.8	242
8	An overview of residual stresses in metal powder bed fusion. Additive Manufacturing, 2019, 27, 131-149.	3.0	228
9	Cotton-Textile-Enabled, Flexible Lithium-Ion Batteries with Enhanced Capacity and Extended Lifespan. Nano Letters, 2015, 15, 8194-8203.	9.1	200
10	Microstructural design of hybrid CoO@NiO and graphene nano-architectures for flexible high performance supercapacitors. Journal of Materials Chemistry A, 2015, 3, 14833-14844.	10.3	177
11	In situ synthesis of ultrafine β-MnO2/polypyrrole nanorod composites for high-performance supercapacitors. Journal of Materials Chemistry, 2011, 21, 10965.	6.7	175
12	High-performance supercapacitors and batteries derived from activated banana-peel with porous structures. Electrochimica Acta, 2016, 222, 1257-1266.	5.2	147
13	Graphene and its derivatives in lithium–sulfur batteries. Materials Today Energy, 2018, 9, 319-335.	4.7	138
14	Towards flexible lithium-sulfur battery from natural cotton textile. Electrochimica Acta, 2017, 246, 507-516.	5.2	137
15	Micro/nanomechanical characterization of ceramic films for microdevices. Thin Solid Films, 1999, 340, 210-217.	1.8	131
16	Bioinspired, Graphene/Al ₂ O ₃ Doubly Reinforced Aluminum Composites with High Strength and Toughness. Nano Letters, 2017, 17, 6907-6915.	9.1	128
17	Mechanical Properties of ZnS Nanobelts. Nano Letters, 2005, 5, 1982-1986.	9.1	121
18	Deformation Strengthening of Biopolymer in Nacre. Advanced Functional Materials, 2011, 21, 3883-3888.	14.9	121

#	Article	IF	CITATIONS
19	Cloning Nacre's 3D Interlocking Skeleton in Engineering Composites to Achieve Exceptional Mechanical Properties. Advanced Materials, 2016, 28, 5099-5105.	21.0	119
20	Ferromagnetic Nanoparticle–Assisted Polysulfide Trapping for Enhanced Lithium–Sulfur Batteries. Advanced Functional Materials, 2018, 28, 1800563.	14.9	109
21	Lithiation-Aided Conversion of End-of-Life Lithium-Ion Battery Anodes to High-Quality Graphene and Graphene Oxide. Nano Letters, 2019, 19, 512-519.	9.1	106
22	B ₄ Câ€Nanowires/Carbonâ€Microfiber Hybrid Structures and Composites from Cotton Tâ€shirts. Advanced Materials, 2010, 22, 2055-2059.	21.0	104
23	Cotton textile enabled, all-solid-state flexible supercapacitors. RSC Advances, 2015, 5, 15438-15447.	3.6	103
24	New Insights into Mossy Li Induced Anode Degradation and Its Formation Mechanism in Li–S Batteries. ACS Energy Letters, 2017, 2, 2696-2705.	17.4	90
25	Unveiling the Formation Mechanism of Pseudo-Single-Crystal Aragonite Platelets in Nacre. Physical Review Letters, 2009, 102, 075502.	7.8	88
26	TaC Nanowire/Activated Carbon Microfiber Hybrid Structures from Bamboo Fibers. Advanced Energy Materials, 2011, 1, 534-539.	19.5	87
27	Uncovering high-strain rate protection mechanism in nacre. Scientific Reports, 2011, 1, 148.	3.3	87
28	Graphene reinforced carbon fibers. Science Advances, 2020, 6, eaaz4191.	10.3	87
29	Reinforcing Mechanisms of Single-Walled Carbon Nanotube-Reinforced Polymer Composites. Journal of Nanoscience and Nanotechnology, 2007, 7, 2309-2317.	0.9	82
30	B4C nanoskeleton enabled, flexible lithium-sulfur batteries. Nano Energy, 2019, 58, 30-39.	16.0	82
31	Micro/nanoscale mechanical and tribological characterization of SiC for orthopedic applications. Journal of Biomedical Materials Research - Part B Applied Biomaterials, 2005, 72B, 353-361.	3.4	81
32	Structural and mechanical characterization of nanoclay-reinforced agarose nanocomposites. Nanotechnology, 2005, 16, 2020-2029.	2.6	81
33	Enhanced nucleate boiling on horizontal hydrophobic-hydrophilic carbon nanotube coatings. Applied Physics Letters, 2013, 102, .	3.3	81
34	Origin of flaw-tolerance in nacre. Scientific Reports, 2013, 3, 1693.	3.3	81
35	Micro/nanomechanical characterization of a natural nanocomposite material—the shell of Pectinidae. Nanotechnology, 2004, 15, 211-217.	2.6	80
36	Capillarity Composited Recycled Paper/Graphene Scaffold for Lithium–Sulfur Batteries with Enhanced Capacity and Extended Lifespan. Small, 2017, 13, 1701927.	10.0	78

#	Article	IF	CITATIONS
37	A generic bamboo-based carbothermal method for preparing carbide (SiC, B4C, TiC, TaC, NbC, TixNb1â^'xC,) T	j ETQ <u>g1</u> 1 0.1	784314 rgB
38	Determination of mechanical properties of Al–Mg alloys dissimilar friction stir welded interface by indentation methods. Journal of Materials Science, 2009, 44, 4140-4147.	3.7	75
39	TiC Nanorods Derived from Cotton Fibers: Chloride-Assisted VLS Growth, Structure, and Mechanical Properties. Crystal Growth and Design, 2011, 11, 4422-4426.	3.0	74
40	Elastic modulus of biopolymer matrix in nacre measured using coupled atomic force microscopy bending and inverse finite element techniques. Materials Science and Engineering C, 2011, 31, 1852-1856.	7.3	71
41	High-temperature delamination mechanisms of thermal barrier coatings: In-situ digital image correlation and finite element analyses. Acta Materialia, 2017, 128, 54-63.	7.9	70
42	Revealing mechanisms of residual stress development in additive manufacturing via digital image correlation. Additive Manufacturing, 2018, 22, 1-12.	3.0	70
43	Carbon Nanotubes Derived from Yeast-Fermented Wheat Flour and Their Energy Storage Application. ACS Sustainable Chemistry and Engineering, 2018, 6, 11386-11396.	6.7	67
44	Size dependency of the elastic modulus of ZnO nanowires: Surface stress effect. Applied Physics Letters, 2007, 91, .	3.3	63
45	Nanoscale structural and mechanical characterization of natural nanocomposites: Seashells. Jom, 2007, 59, 71-74.	1.9	62
46	Predicting Young's modulus of nanowires from first-principles calculations on their surface and bulk materials. Journal of Applied Physics, 2008, 104, .	2.5	60
47	Converting eggs to flexible, all-solid supercapacitors. Nano Energy, 2019, 65, 104045.	16.0	60
48	In situ defect detection in selective laser melting via full-field infrared thermography. Additive Manufacturing, 2018, 24, 595-605.	3.0	59
49	Deformation and fracture behaviors of microporous polymer separators for lithium ion batteries. RSC Advances, 2014, 4, 14904.	3.6	57
50	Bioinspired, graphene-enabled Ni composites with high strength and toughness. Science Advances, 2019, 5, eaav5577.	10.3	55
51	Low-temperature carbonization of polyacrylonitrile/graphene carbon fibers: A combined ReaxFF molecular dynamics and experimental study. Carbon, 2021, 174, 345-356.	10.3	55
52	Uncovering Aragonite Nanoparticle Self-assembly in Nacre—A Natural Armor. Crystal Growth and Design, 2012, 12, 4306-4310.	3.0	53
53	Cotton-Derived Fe/Fe ₃ C-Encapsulated Carbon Nanotubes for High-Performance Lithium–Sulfur Batteries. Nano Letters, 2022, 22, 1217-1224.	9.1	51
54	Low temperature, organic-free synthesis of Ba ₃ B ₆ O ₉ (OH) ₆ nanorods and β-BaB ₂ O ₄ nanospindles. Journal of Materials Chemistry, 2009, 19, 983-987.	6.7	50

#	Article	IF	CITATIONS
55	Determination of interfacial properties of thermal barrier coatings by shear test and inverse finite element method. Acta Materialia, 2010, 58, 5972-5979.	7.9	50
56	Tobacco mosaic virus templated synthesis of one dimensional inorganic–polymer hybrid fibres. Journal of Materials Chemistry, 2009, 19, 2841.	6.7	48
57	Prediction of microstructural defects in additive manufacturing from powder bed quality using digital image correlation. Materials Science & Engineering A: Structural Materials: Properties, Microstructure and Processing, 2020, 794, 140002.	5.6	48
58	Nanoindentation for measuring individual phase mechanical properties of lead free solder alloy. Journal of Materials Science: Materials in Electronics, 2008, 19, 514-521.	2.2	47
59	B/SiO _{<i>x</i>} Nanonecklace Reinforced Nanocomposites by Unique Mechanical Interlocking Mechanism. Advanced Materials, 2008, 20, 4091-4096.	21.0	47
60	Electrospinning fabrication, structural and mechanical characterization of rod-like virus-based composite nanofibers. Journal of Materials Chemistry, 2011, 21, 8550.	6.7	47
61	Hidden energy dissipation mechanism in nacre. Journal of Materials Research, 2014, 29, 1573-1578.	2.6	47
62	Plastic Deformation Enabled Energy Dissipation in a Bionanowire Structured Armor. Nano Letters, 2014, 14, 2578-2583.	9.1	47
63	Sample size effect on nanoindentation of micro-/nanostructures. Acta Materialia, 2006, 54, 1699-1703.	7.9	46
64	Adhesion at diamond/metal interfaces: A density functional theory study. Journal of Applied Physics, 2010, 107, .	2.5	46
65	Microindentation test for assessing the mechanical properties of cartilaginous tissues. Journal of Biomedical Materials Research - Part B Applied Biomaterials, 2007, 80B, 25-31.	3.4	45
66	The effect of protein adsorption on the friction behavior of ultra-high molecular weight polyethylene. Tribology Letters, 2006, 22, 181-188.	2.6	41
67	Nanoscale structural and mechanical characterization of heat treated nacre. Materials Science and Engineering C, 2009, 29, 1803-1807.	7.3	41
68	Order-Disorder Transition of Aragonite Nanoparticles in Nacre. Physical Review Letters, 2012, 109, 025501.	7.8	40
69	Tailoring nanocomposite interfaces with graphene to achieve high strength and toughness. Science Advances, 2020, 6, .	10.3	40
70	Elastic modulus of single-crystal GaN nanowires. Journal of Materials Research, 2006, 21, 2882-2887.	2.6	39
71	Multiscale hierarchical assembly strategy and mechanical prowess in conch shells (Busycon carica). Journal of Structural Biology, 2013, 184, 409-416.	2.8	39
72	Exploring the Energy Storage Mechanism of High Performance MnO ₂ Electrochemical Capacitor Electrodes: An In Situ Atomic Force Microscopy Study in Aqueous Electrolyte. Advanced Functional Materials, 2013, 23, 4745-4751.	14.9	39

Xiaodong Li

#	Article	IF	CITATIONS
73	Quantifying the three-dimensional damage and stress redistribution mechanisms of braided SiC/SiC composites by in situ volumetric digital image correlation. Scripta Materialia, 2017, 130, 238-241.	5.2	37
74	Unveiling Carbon Ring Structure Formation Mechanisms in Polyacrylonitrile-Derived Carbon Fibers. ACS Applied Materials & Interfaces, 2019, 11, 42288-42297.	8.0	36
75	In Situ Nanoscale In-Plane Deformation Studies of Ultrathin Polymeric Films During Tensile Deformation Using Atomic Force Microscopy and Digital Image Correlation Techniques. IEEE Nanotechnology Magazine, 2007, 6, 4-12.	2.0	35
76	Synthesis, structural, optical and mechanical characterization of SrB2O4 nanorods. CrystEngComm, 2011, 13, 5858.	2.6	34
77	Twin boundary spacing-dependent friction in nanotwinned copper. Physical Review B, 2012, 85, .	3.2	34
78	Structural and Mechanical Characterization of Thermally Treated Conch Shells. Jom, 2015, 67, 720-725.	1.9	30
79	Predicting the hydrogen pressure to achieve ultralow friction at diamond and diamondlike carbon surfaces from first principles. Applied Physics Letters, 2008, 92, .	3.3	29
80	Unveiling residual stresses in air plasma spray coatings by digital image correlation. Extreme Mechanics Letters, 2016, 7, 126-135.	4.1	29
81	Nanomechanical characterization of polyaniline coated tobacco mosaic virus nanotubes. Journal of Biomedical Materials Research - Part A, 2008, 87A, 8-14.	4.0	28
82	Mapping nanoscale wear field by combined atomic force microscopy and digital image correlation techniques. Acta Materialia, 2008, 56, 6304-6309.	7.9	28
83	Uniting Strength and Toughness of Al Matrix Composites with Coordinated Al ₃ Ni and Al ₃ Ti Reinforcements. Advanced Engineering Materials, 2018, 20, 1700605.	3.5	28
84	Recent advances in biomass-derived graphene and carbon nanotubes. Materials Today Sustainability, 2022, 18, 100138.	4.1	27
85	Dynamic self-strengthening of a bio-nanostructured armor — conch shell. Materials Science and Engineering C, 2019, 103, 109820.	7.3	26
86	Damage mechanisms in elastomeric foam composites: Multiscale X-ray computed tomography and finite element analyses. Composites Science and Technology, 2019, 169, 195-202.	7.8	26
87	Atomistic Origin of Deformation Twinning in Biomineral Aragonite. Physical Review Letters, 2017, 118, 105501.	7.8	25
88	Converting PBO fibers into carbon fibers by ultrafast carbonization. Carbon, 2020, 159, 432-442.	10.3	25
89	Carbon fibers derived from commodity polymers: A review. Carbon, 2022, 196, 422-439.	10.3	24
90	A biopolymer-like metal enabled hybrid material with exceptional mechanical prowess. Scientific Reports, 2015, 5, 8357.	3.3	23

#	Article	IF	CITATIONS
91	Atomistic investigation of scratching-induced deformation twinning in nanocrystalline Cu. Journal of Applied Physics, 2012, 112, .	2.5	21
92	In situ observation of fracture behavior of canine cortical bone under bending. Materials Science and Engineering C, 2016, 62, 361-367.	7.3	21
93	Bioinspired, Multiscale Reinforced Composites with Exceptionally High Strength and Toughness. Nano Letters, 2018, 18, 5812-5820.	9.1	21
94	In Situ Observation of Small-Scale Deformation in a Lead-Free Solder Alloy. Journal of Electronic Materials, 2009, 38, 400-409.	2.2	20
95	Upcycling of paper waste for high-performance lithium-sulfur batteries. Materials Today Energy, 2021, 19, 100591.	4.7	20
96	Analysis of tow architecture variability in biaxially braided composite tubes. Composites Part B: Engineering, 2020, 190, 107938.	12.0	19
97	Whisker nucleation in indentation residual stress field on tin plated component leads. Journal of Materials Science: Materials in Electronics, 2007, 18, 599-604.	2.2	18
98	Yeast-Derived Carbon Nanotube-Coated Separator for High Performance Lithium-Sulfur Batteries. Jom, 2021, 73, 2516-2524.	1.9	17
99	Approaching Carbon Nanotube Reinforcing Limit in B ₄ <scp>C</scp> Matrix Composites Produced by Chemical Vapor Infiltration. Advanced Engineering Materials, 2014, 16, 161-166.	3.5	16
100	Atomic-scale imaging correlation on the deformation and sensing mechanisms of SnO2 nanowires. Applied Physics Letters, 2014, 105, .	3.3	15
101	The Art of Curved Reinforcing in Biological Armors — Seashells. Journal of Bionic Engineering, 2019, 16, 711-718.	5.0	15
102	Unveiling damage mechanisms of chromium-coated zirconium-based fuel claddings by coupling digital image correlation and acoustic emission. Materials Science & Engineering A: Structural Materials: Properties, Microstructure and Processing, 2020, 774, 138850.	5.6	15
103	Low energy electroplasticity in aluminum alloys. Materials Science & Engineering A: Structural Materials: Properties, Microstructure and Processing, 2020, 798, 140235.	5.6	15
104	Hard-particle rotation enabled soft–hard integrated auxetic mechanical metamaterials. Proceedings of the Royal Society A: Mathematical, Physical and Engineering Sciences, 2019, 475, 20190234.	2.1	14
105	Unveiling hermetic failure of ceramic tubes by digital image correlation and acoustic emission. Journal of the American Ceramic Society, 2020, 103, 2146-2159.	3.8	13
106	Quantifying the effect of tow architecture variability on the performance of biaxially braided composite tubes. Composites Part B: Engineering, 2020, 201, 108383.	12.0	13
107	Internal Electron Tunneling Enabled Ultrasensitive Position/Force Peapod Sensors. Nano Letters, 2015, 15, 7281-7287.	9.1	11
108	Scalable measurements of tow architecture variability in braided ceramic composite tubes. Journal of the American Ceramic Society, 2018, 101, 4297-4307.	3.8	11

#	Article	IF	CITATIONS
109	Nano/micro-mechanical and tribological characterization of Ar, C, N, and Ne ion-implanted Si. Journal of Materials Research, 2010, 25, 880-889.	2.6	10
110	In Situ Observation of Fracture Behavior of Bamboo Culm. Jom, 2021, 73, 1705-1713.	1.9	10
111	A new approach for the preparation of variable valence rare earth alloys from nano rare earth oxides at a low temperature in molten salt. RSC Advances, 2012, 2, 1585-1591.	3.6	9
112	Structural and elastic properties of InN nanowires. Physica Status Solidi (A) Applications and Materials Science, 2012, 209, 718-723.	1.8	9
113	Unveiling polytype transformation assisted growth mechanism in boron carbide nanowires. Journal of Crystal Growth, 2018, 481, 11-17.	1.5	9
114	Characterizing environmentâ€dependent fracture mechanisms of ceramic matrix composites via digital image correlation. Journal of the American Ceramic Society, 2021, 104, 6545-6562.	3.8	9
115	Particle clustering effects on damage mechanisms in elastomeric syntactic foams. Composites Part B: Engineering, 2019, 175, 107160.	12.0	8
116	Analysis of SiC/SiC composites for energy applications at ambient conditions. Journal of the American Ceramic Society, 2021, 104, 481-491.	3.8	8
117	Influence of Scanning Rotation on Nanoscale Artificial Strain in Open-Loop Atomic Force Microscopy. Experimental Mechanics, 2011, 51, 619-624.	2.0	7
118	3D digital image correlation evaluation of arthrodesis implants. Clinical Biomechanics, 2020, 71, 29-36.	1.2	7
119	Sliding Probe Methods for <italic>In Situ</italic> Nanorobotic Characterization of Individual Nanostructures. IEEE Transactions on Robotics, 2015, 31, 12-18.	10.3	6
120	Interfacial modification of amorphous substrates for microcrystalline silicon growth within situ hydrogen plasma pretreatment. Physica Status Solidi A, 2005, 202, 2448-2453.	1.7	5
121	Probing the local creep mechanisms of SiC/SiC ceramic matrix composites with high-temperature nanoindentation. Journal of Materials Research, 2021, 36, 2420-2433.	2.6	5
122	Unveiling damage mechanisms of chromium-coated zirconium-based fuel claddings at LWR operating temperature by in-situ digital image correlation. Surface and Coatings Technology, 2022, 429, 127909.	4.8	5
123	Mechanically robust Si nanorod arrays on Cu/Ti bilayer film coated Si substrate for high performance lithium-ion battery anodes. Journal of Applied Physics, 2012, 112, .	2.5	4
124	Unveiling Ultra-High Temperature Wear and Indentation Damage Mechanisms of Thermal Barrier Coatings. Jom, 2015, 67, 2921-2933.	1.9	4
125	Multiple-objective motion planning for unmanned aerial vehicles. , 2011, , .		4
126	Enhance diamond coating adhesion by oriented interlayer microcracking. Journal of Applied Physics, 2009, 106, 123514.	2.5	2

#	Article	IF	CITATIONS
127	In situ electrical property characterization of individual nanostructures using a sliding probe inside a transmission electron microscope. , 2010, , .		2
128	Size and Crystal Orientation-Dependent Thermal Behaviors of ZnO Nanobelts. Journal of Physical Chemistry C, 2020, 124, 27222-27229.	3.1	2
129	Multiple robot simultaneous localization and mapping. , 2011, , .		2

	Carbon Nanotubes: Hydrogen I	Passivation Induced Dispersion of	Multi-Walled Carbon Nanotube	s (Adv.) Ti ETOaO () () rgBT /()verlock 10
130		Passivation Induced Dispersion of		(,, .) <u>=</u> . eqe	21.0	1

131	AFM Imaging of Water, Cells and Tissues. Materials Research Society Symposia Proceedings, 2005, 874, 1.	0.1	0
132	Polycrystalline Si1-xGex thin film deposition by rapid thermal chemical vapor deposition. Journal of Materials Science: Materials in Electronics, 2006, 17, 27-33.	2.2	0
133	Nanoclay-reinforced Polyacrylamide Composite: Synthesis, Structural and Mechanical Characterization. Materials Research Society Symposia Proceedings, 2009, 1239, 1.	0.1	0
134	Nanomechanical Measurements in Harsh Environments. Jom, 2015, 67, 2900-2901.	1.9	0
135	Modeling and simulation of an ultrasensitive electron tunneling position/force nanosensor. RSC Advances, 2016, 6, 8297-8302.	3.6	0